PHYSICAL REVIEW B **75**, 020511(R) (2007)

Anisotropic gap of superconducting CaC_6: A first-principles density functional calculation

A. Sanna,[1] G. Profeta,[1] A. Floris,[2] A. Marini,[3] E. K. U. Gross,[2] and S. Massidda[1]

[1]*SLACS-INFM/CNR, Sardinian Laboratory for Computational Materials Science and Dipartimento di Scienze Fisiche, Università degli Studi di Cagliari, Cagliari, Italy*

[2]*Institut für Theoretische Physik, Freie Universität Berlin, Arnimallee 14, D-14195 Berlin, Germany*

[3]*Physics Department, University of Rome "Tor Vergata," Rome, Italy*

(Received 11 August 2006; published 30 January 2007)

We report first-principles calculations of the superconducting properties of CaC_6, obtained within the density functional theory of superconductivity. We find a moderately anisotropic gap which is larger on the Fermi surface sheet with interlayer and Ca character compared with isotropic calculations. Our calculated anisotropy improves the agreement with specific heat experiments and is consistent with recent tunneling experiments. In contrast to MgB_2, we do not find multigap superconductivity but, instead, a continuous spread of gap values.

DOI: 10.1103/PhysRevB.75.020511 PACS number(s): 74.25.Jb, 74.25.Kc, 74.70.Ad

Graphite intercalated compounds (GICs) were first found to be superconductors in 1965.[1] Doping with Li,[2] Na,[3] and K,[1] however, produced superconductivity only at low temperatures around 1 K. During the past year, GICs have enjoyed renewed attention after the discovery of superconductivity in CaC_6 and YbC_6 at 11.5 and 6.5 K,[4,5] respectively. From the theoretical point of view, the most important question is related to the pairing mechanism active in these compounds. *Ab initio* calculations[6,7] of the electronic and dynamical properties of CaC_6 have pointed out that electron-phonon (*e*-ph) coupling is sufficient to yield the observed T_c. The phonons mostly contributing to superconductivity belong to an optical branch involving Ca displacements and, to a lower extent, to two C-related branches at a much higher frequency. However, despite these detailed investigations, some aspects have remained unsolved;[8,9] in particular, (i) the experimental specific heat behavior[10] was first interpreted as an indication of isotropic one-gap BCS superconductivity, but this interpretation was later questioned;[8] (ii) experimental results on the isotopic effect, a clear indication of the *e*-ph mechanism, report a large Ca isotope coefficient ($\approx$0.5), while *ab initio* calculations based on the McMillan equation report a much lower value ($\approx$0.25). These problems were used to discuss the possibility of anisotropic superconductivity.[8]

In fact, the electronic structure of CaC_6 around the Fermi level (E_F) is quite rich. Together with nearly two-dimensional C π bands, there is a three-dimensional band with a free-electron-like behavior. In the absence of intercalated atoms, this band persists with a strong interlayer character (but becomes unoccupied). Interlayer bands, uncorrelated with a particular atomic orbital, have been discussed extensively in graphite,[11] GICs,[6,9,11–13] and MgB_2.[14] In CaC_6 however, this band gains a further strong contribution from Ca 4*s* and 3*d* orbitals. This band is coupled to the Ca optical in-plane phonon branch; these low-frequency modes provide a strong contribution to the *e*-ph constant λ.[6,7] In this situation, therefore, it is quite natural to question the isotropy of superconducting properties.

In this Rapid Communication, we report *ab initio* calculations of anisotropic superconductivity in CaC_6. Our calculations are based on density functional theory for the superconducting state[15,16] (SCDFT), which was successfully employed to describe superconductivity in elemental metals, MgB_2,[14] and Li, Al, and K under pressure.[17,18] Unlike common Eliashberg approaches, we do not need any *ad hoc* parameter such as μ^*. Generalized to a fully **k**-point-resolved implementation, the unique capabilities of the method are used here to obtain a detailed analysis of the superconducting energy gap and of the electron-phonon coupling over the Fermi surface (FS). We also investigate the role of different intraband and interband Coulomb repulsion terms. We use our results to (i) interpret the experimental temperature dependence of the specific heat in CaC_6 and work out the contribution of the gap anisotropy by model calculations, (ii) calculate the isotope effect coefficients ($\alpha_X, X=\mathrm{Ca,C}$), and (iii) discuss the tunneling experiments.[19]

The implementation of SCDFT has been reported elsewhere,[15,16] and we give here only a very brief summary. The central equation of the DFT for superconductors is a generalized gap equation of the form

$$\Delta_{n\mathbf{k}} = -\mathcal{Z}_{n\mathbf{k}}\Delta_{n\mathbf{k}} - \frac{1}{2}\sum_{n'\mathbf{k}'} \mathcal{K}_{n\mathbf{k},n'\mathbf{k}'} \frac{\tanh\left(\frac{\beta}{2}E_{n'\mathbf{k}'}\right)}{E_{n'\mathbf{k}'}}\Delta_{n'\mathbf{k}'}, \quad (1)$$

where n and $\mathbf{k}$, respectively, are the electronic band index and the wave vector inside the Brillouin zone. β is the inverse temperature and $E_{n\mathbf{k}}=\sqrt{(\varepsilon_{n\mathbf{k}}-\mu)^2+|\Delta_{n\mathbf{k}}|^2}$ are the excitation energies of the superconductor, defined in terms of the gap function $\Delta_{n\mathbf{k}}$, the Kohn-Sham eigenenergies of the normal-state band structure $\varepsilon_{n\mathbf{k}}$, and the chemical potential μ. The kernel $\mathcal{K}$ appearing in the gap equation consists of two contributions $\mathcal{K}=\mathcal{K}^{e\text{-ph}}+\mathcal{K}^{e\text{-}e}$, representing the effects of the *e*-ph and *e*-*e* interactions, respectively. $\mathcal{K}^{e\text{-ph}}_{n\mathbf{k},n'\mathbf{k}'}$ and $\mathcal{Z}_{n\mathbf{k}}$ are matrix elements with respect to Kohn-Sham Bloch functions of the exchange-correlation (XC) functional associated with the electron-phonon interaction while $\mathcal{K}^{e\text{-}e}_{n\mathbf{k},n'\mathbf{k}'}$ are the corresponding matrix elements of the purely electronic (superconducting) XC functional.[20] The simplest approximation for the latter is a screened Coulomb interaction which, in the following calculations, includes nondiagonal effects within the random phase approximation (RPA). As in the case MgB_2,[14] a diagonal screening leads to sizable differences, as expected for open, covalently bonded structures. In the present formulation, the full anisotropy of the kernel $\mathcal{K}_{n\mathbf{k},n'\mathbf{k}'}$

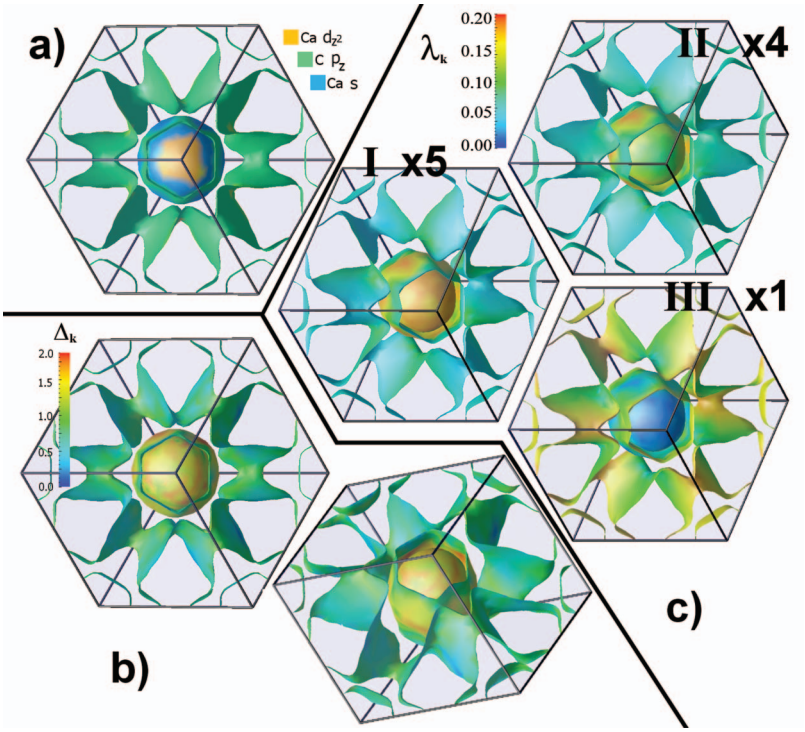

FIG. 1. (Color) Fermi surfaces of CaC_6, with a color coding indicating (a) the larger contribution to the charge projection; (b) superconducting gap; (c) $\lambda_{n\mathbf{k}}$ summed over the three major groups of phonon modes; the number indicates the factor by which one should multiply the value read in the scale.

is maintained, which results in a band- and **k**-dependent superconducting gap over the FSs. However, the Coulomb part does not contribute significantly to anisotropy.

Ground-state properties and electronic structure calculations were performed using the pseudopotential-based code[21] PWSCF within the Perdew-Wang[22] generalized gradient approximation for the (normal-conducting) XC functional. Ultrasoft pseudopotentials have been used with Ca $3s$ and $3p$ states in valence, and with 30 and 300 Ry cutoffs in the plane-wave expansion of wave functions and charge density, respectively. Phonon frequencies and e-ph couplings were obtained from density functional perturbation theory on a $6\times6\times6$ **q** mesh. Test calculations have shown that a $6\times6\times6$ **k**-point mesh for electronic integration, with a Methfessel-Paxton smearing width of 0.06 Ry, is sufficient to provide frequencies and couplings converged within 2% at Γ. The electron-phonon spectral function $\alpha^2F(\Omega)$ and **k**-dependent $\lambda_{n\mathbf{k}}$ were evaluated through a careful integration over the Fermi surface, starting from a $10\times10\times10$ **k**-point mesh of calculated e-ph matrix elements ($g^{j\mathbf{q}}_{n\mathbf{k}n'\mathbf{k}'}$, where j is the phonon branch index and $\mathbf{q}=\mathbf{k}-\mathbf{k}'$ is the phonon wave vector) and interpolating on the FS. The statically screened Coulomb potential has been calculated including nondiagonal effects within the RPA, using the SELF code.[23]

As the electronic structure of CaC_6 has already been described by Calandra and Mauri[6] and by Mazin *et al.*,[13] we only sketch here the main points. The C σ bands are completely filled, and at the Fermi level only the C π bands are present, forming two-dimensional, wrapped cylindrical FS sheets running along the direction perpendicular to the graphene layers. However, we also find a part of the FS forming from the interlayer bands. In CaC_6 these states are strongly mixed with Ca s and d_{z^2} states; the latter orbitals, empty in atomic Ca, are partially occupied in the solid. These states form an almost spherical FS, intersecting the C π FS. Because of the **k**-point-dependent mixing, the nature of electron states changes in the different FS sheets but also within each sheet. Clearly, this situation suggests the possibility of a strongly **k**-dependent superconducting gap.

In Fig. 1(a) we show the dominant orbital character over the Fermi surface. We see that, while C π states are dominant and homogeneous on the tubular FS structures (with a minor contribution from d_{xy} and $d_{x^2-y^2}$ Ca states, $\approx1/3$ of the total charge), Ca orbitals contribute anisotropically on the internal, spherical FS: the d_{z^2} components dominate on the portions oriented along the directions perpendicular to the graphene planes, whereas on the remaining parts of the FS a mixture of s and interlayer states dominates. The tubular and spherical FSs mix on the intersection regions, but the mixing is small.

Both the phonon bands and the Eliashberg function (leading to an electron-phonon coupling constant $\lambda=0.85\pm0.02$) are in good agreement with previous calculations.[6] Solving Eq. (1) for the superconducting gap $\Delta_{n\mathbf{k}}$ as a function of T, we calculate the critical temperature. We obtain $T_c^{calc}\approx9.4$ K, in good agreement with the experimental value $T_c^{expt}=11.5$ K. We emphasize in this context that our calculations have no adjustable parameter, and that the superconducting properties have an intrinsically exponential dependence on the couplings, which makes an accurate calculation of T_c a hard task.

Figure 1(b) shows, under two different perspectives, the $T=0$ K superconducting gap, $\Delta_{n\mathbf{k}}$, on the different parts of the FS; its energy dependence away from E_F is illustrated in Fig. 2. We clearly see a correlation between the orbital character of states and $\Delta_{n\mathbf{k}}$, which is larger for the Ca-dominated FS. Furthermore, we notice the presence of some anisotropy on the individual FS sheets; in particular, the region close to

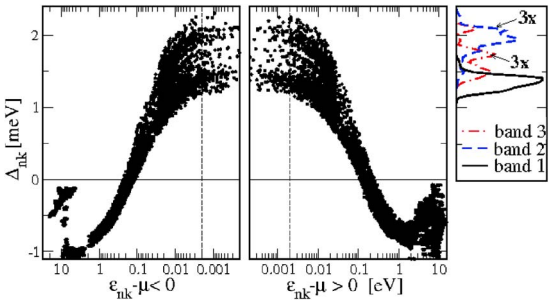

FIG. 2. (Color online) Superconducting gap as a function of energy. The right panel shows the gap distribution on the three bands within 2 meV from E_F (see text); band 2 and band 3 plots are multiplied by a factor of 3.

the intersection between tubular and spherical parts shows the largest variations.

This structure of the superconducting gap $\Delta_{n\mathbf{k}}$ is mainly due to the different electron-phonon couplings on the FS sheets. We define

$$\lambda_{n\mathbf{k}j} = 2\sum_{n'\mathbf{k}'} \frac{|g^{j\mathbf{q}}_{n\mathbf{k}n'\mathbf{k}'}|^2}{\omega_{j\mathbf{q}}} \delta(\varepsilon_{n'\mathbf{k}'} - \mu). \quad (2)$$

Figure 1(c) shows the $\lambda_{n\mathbf{k}_F j}$ summed over j belonging to three main groups of peaks in the phononic density of states, i.e., the group of soft Ca modes (I) centered at about 15 meV; that of out-of-plane C modes (II) at ~60 meV; and that of C in-plane modes (III) at 170 meV. The first and (to a lesser extent) second groups give a large contribution to the global coupling with the interlayer band (spherical FS); while the Ca modes give a roughly homogeneous coupling, the C out-of-plane modes (group II) interact mainly with the s region of this part of the Fermi surface. The C in-plane modes give a contribution to the global coupling which is a factor of 4 smaller[6] and, as expected, these modes couple strictly with C states.

The energy-dependent distribution of $\Delta_{n\mathbf{k}}$ in Fig. 2 emphasizes more clearly this anisotropy. To each isoenergy surface corresponds a large spread of $\Delta_{n\mathbf{k}}$: The largest and the smallest values differs roughly by a factor of 2, smaller than the difference between σ and π gaps in MgB_2 but far from negligible. Unlike in MgB_2, we have a continuum of gap values; their average value, 1.63 meV, compares well with experiments giving 1.79 (Ref. 25) and 1.6 eV (Ref. 19) by penetration depth and scanning tunneling microscope (STM) measurements, respectively. In the remaining part of this Rapid Communication, we will focus on the peculiarities and consequences of this anisotropy. The right panel of Fig. 2 shows the distribution of gap values over the three bands crossing E_F, separated to the largest possible extent into physically distinct regions. The outer π FS (band 1) has a small spread around the minimum of $\Delta_{n\mathbf{k}}$. The spherical FS (band 2) has the largest values, and the π FS crossing the spheres (band 3) lies in between the other two. A minimum appears in the distribution, but no separation into two gaps results.

Away from E_F, $\Delta_{n\mathbf{k}}$ changes sign.[14–16] While the exact behavior of $\Delta_{n\mathbf{k}}$ far from E_F becomes progressively less important, due to the energy denominator in Eq. (1), the negative tail of the gap provides the basic mechanism leading to the renormalization of the e-e repulsion. In particular, in the negative energy region (occupied valence bands), the σ bands correspond to (negative) values of $\Delta_{n\mathbf{k}}$ considerably smaller in absolute value than the values on the occupied π bands. Referring to Eq. (1), the reason is the following. In this region the absolute value of the gap is increased only by the interband Coulomb repulsion between C σ and both C π and Ca s, d_{z^2}–C σ states near E_F; at the same time, it is decreased by the stronger intraband C σ-σ Coulomb repulsion, which is much stronger than the intraband π-π repulsion. A similar analysis can be done for the π gap close to E_F: apart from the (attractive) phononic term, concerning the Coulomb contributions Δ_π is increased by the interband π-σ interaction, and decreased by intraband π-π and interband π–Ca s, d_{z^2} terms. We point out here that this anisotropy of interactions, which is the cause of the gap anisotropy, is very important in the calculation of the critical temperature: An averaged, free-electron-like description of Coulomb matrix elements leads to a higher value of the critical temperature (as in MgB_2, although to a lesser extent).

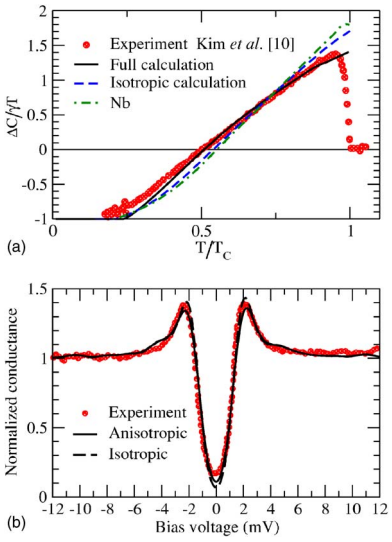

FIG. 3. (Color online) Upper panel: Reduced specific heat of CaC_6. Lower panel: experimental normalized conductance compared to the ratio between superconducting and normal state DOS.

In Fig. 3(a) we plot the temperature dependence of the difference between the superconducting and normal specific heats of CaC_6, compared with experiment. To avoid the amplification of differences between experimental and theoretical T_c and Sommerfeld constant γ, we normalize T and C/T, respectively, to T_c and γ (both experimental and theoretical). Our calculations (full black curve) compare rather well with experiment, basically in the whole temperature range. The discontinuity at T_c is quite close to the BCS value $\Delta C = 1.43\gamma T_c$, as expected in the presence of medium coupling strength. Specific heat data were originally[10] used to argue for an isotropic superconducting order parameter, and later questioned by Mazin *et al.*,[8] who found that the experimental specific heat cannot be reconciled with the isotropic model.

To investigate this point further, we performed a calculation of the specific heat using isotropically averaged interactions. We can see that the corresponding results show a clear discrepancy from experiment, much larger than that of the anisotropic calculation, with a general shape quite similar to the one found in the calculations by Mazin *et al.*[8] In particular, in the low-temperature region the isotropic results are too low compared with experiments. To investigate this point further, we plot in Fig. 3(a) similar data for Nb. It turns out that, when properly renormalized, the same general trend is common to these isotropic calculations, with some obvious differences due to the strength of the coupling (jump at T_c).

Isotope effect coefficients (IECs) were calculated from the McMillan equation by Calandra and Mauri,[6] who obtained $\alpha_{\mathrm{Ca}}=0.24$ and $\alpha_{\mathrm{C}}=0.26$, where $\alpha_X=-(d\log T_c/d\log M_X)$. However, recent experiments by Hinks *et al.*[24] give a much larger Ca IEC, in the range 0.4–0.56. We performed a calculation of the IECs from the variation of the critical temperature with Ca and C isotope masses. In principle, in our formalism, unlike in the McMillan formula with a fixed μ^*, there is an additional contribution to the IEC due to the renormalization of the Coulomb interaction that depends on the position of the gap node. The latter in turn is affected by the isotope masses. Still, we find $\alpha_{\mathrm{Ca}}=0.23$ and $\alpha_{\mathrm{C}}=0.24$, in agreement with the McMillan results obtained both in previous calculations[6] and in our work. This discrepancy, which could be justified by the presence of strong anharmonic effects, also calls for further experiments on IECs.

Scanning tunneling microscopy experiments have been recently performed[19] on polycrystalline CaC_6 films oriented along the *c* axis. These films showed a slightly reduced gap (by accident nearly equal to our averaged value) and T_c. According to the authors, the tunneling current should come mainly from the Ca-related three-dimensional spherical FS, but this analysis could be modified by several experimental effects. They could obtain a good fit of experiments by smearing a BCS single-gap curve with a 0.2 meV broadening. Figure 3(b) shows the experimental data, together with our results, obtained by calculating the superconducting density of states (DOS), normalized to the normal-state DOS and filtered with a thermal broadening similar to the experimental one. We use both the anisotropic gap results and its average over isoenergy surfaces. The agreement is pretty good, apart from the two bumps at ±5 meV, which depend on the computational details (e.g., FS sampling) and are equal in the anisotropic and isotropic calculations. In agreement with Ref. 19, we conclude that the experimental results can be equally well reproduced using an anisotropic gap, or by a larger smearing of a BCS isotropic curve, originating from experimental reasons. Clearly, we do not have two distinct gaps.

In conclusion, by means of a fully *ab initio* approach we have calculated the superconducting properties of CaC_6. The experimental T_c, specific heat, STM, and isotope effect are well described assuming a conventional electron-phonon coupling. We find a continuous spread of gap values, i.e., multigap superconductivity is clearly ruled out by our calculations. However, there is a sizable anisotropy in the interactions leading to an anisotropic gap over the Fermi surface compatible with the present experimental situation.

We thank I. Mazin and L. Boeri for fruitful discussions. This work was partially supported by the Italian Ministry of Education, through PRIN 2006021741 and PON-CyberSar, by the Istituto Nazionale di Fisica della Materia (INFM-CNR) through a supercomputing grant at Cineca (Bologna, Italy), by the Deutsche Forschungsgemeinschaft, and by the NANOQUANTA Network of Excellence.

[1] N. B. Hannay *et al.*, Phys. Rev. Lett. **14**, 225 (1965).
[2] I. Belash *et al.*, Solid State Commun. **69**, 921 (1989).
[3] V. Avdeev *et al.*, Pis'ma Zh. Eksp. Teor. Fiz. **43**, 376 (1986).
[4] T. E. Weller *et al.*, Nat. Phys. **1**, 39 (2005).
[5] N. Emery, C. Herold, M. d'Astuto, V. Garcia, C. Bellin, J. F. Mareche, P. Lagrange, and G. Loupias, Phys. Rev. Lett. **95**, 087003 (2005).
[6] M. Calandra and F. Mauri, Phys. Rev. Lett. **95**, 237002 (2005).
[7] J. S. Kim, L. Boeri, R. K. Kremer, and F. S. Razavi, Phys. Rev. B **74**, 214513 (2006).
[8] I. I. Mazin *et al.*, cond-mat/0606404 (unpublished).
[9] M. Calandra and F. Mauri, Phys. Rev. B **74**, 094507 (2006).
[10] J. S. Kim, R. K. Kremer, L. Boeri, and F. S. Razavi, Phys. Rev. Lett. **96**, 217002 (2006).
[11] M. Posternak, A. Baldereschi, A. J. Freeman, E. Wimmer, and M. Weinert, Phys. Rev. Lett. **50**, 761 (1983).
[12] G. Csányi *et al.*, Nat. Phys. **1**, 42 (2005).
[13] I. I. Mazin, Phys. Rev. Lett. **95**, 227001 (2005).
[14] A. Floris, G. Profeta, N. N. Lathiotakis, M. Lüders, M. A. L. Marques, C. Franchini, E. K. U. Gross, A. Continenza, and S. Massidda, Phys. Rev. Lett. **94**, 037004 (2005).
[15] M. Lüders, M. A. L. Marques, N. N. Lathiotakis, A. Floris, G. Profeta, L. Fast, A. Continenza, S. Massidda, and E. K. U. Gross, Phys. Rev. B **72**, 024545 (2005).
[16] M. A. L. Marques, M. Lüders, N. N. Lathiotakis, G. Profeta, A. Floris, L. Fast, A. Continenza, E. K. U. Gross, and S. Massidda, Phys. Rev. B **72**, 024546 (2005).
[17] G. Profeta, C. Franchini, N. N. Lathiotakis, A. Floris, A. Sanna, M. A. L. Marques, M. Lüders, S. Massidda, E. K. U. Gross, and A. Continenza, Phys. Rev. Lett. **96**, 047003 (2006).
[18] A. Sanna, C. Franchini, A. Floris, G. Profeta, N. N. Lathiotakis, M. Lüders, M. A. L. Marques, E. K. U. Gross, A. Continenza, and S. Massidda, Phys. Rev. B **73**, 144512 (2006).
[19] N. Bergeal, V. Dubost, Y. Noat, W. Sacks, D. Roditchev, N. Emery, C. Herold, J. Marêché, P. Lagrange, and G. Loupias, Phys. Rev. Lett. **97**, 077003 (2006).
[20] S. Kurth, M. Marques, M. Lüders, and E. K. U. Gross, Phys. Rev. Lett. **83**, 2628 (1999)
[21] S. Baroni *et al.*, http://www.pwscf.org/
[22] J. P. Perdew and Y. Wang, Phys. Rev. B **45**, 13244 (1992).
[23] A. Marini *et al.*, the SELF project code, http://www.fisica.uniroma2.it/~self/
[24] D. G. Hinks, D. Rosenmann, H. Claus, M. S. Bailey, and J. D. Jorgensen, Phys. Rev. B **75**, 014509 (2007).
[25] G. Lamura, M. Aurino, G. Cifariello, E. Di Gennaro, A. Andreone, N. Emery, C. Hérold, J.-F. Marêché, and P. Lagrange, Phys. Rev. Lett. **96**, 107008 (2006).